# Environmental Science Processes & Impacts



### **PAPER**

View Article Online
View Journal



Cite this: DOI: 10.1039/c8em00291f

# Degradation of polyethylene glycols and polypropylene glycols in microcosms simulating a spill of produced water in shallow groundwater†

Jessica D. Rogers, Dab E. Michael Thurman, Da Imma Ferrer, Da James S. Rosenblum, Morgan V. Evans, Dc Paula J. Mouser Cd and Joseph N. Ryan Na Ryan Na

Polyethylene glycols (PEGs) and polypropylene glycols (PPGs) are frequently used in hydraulic fracturing fluids and have been detected in water returning to the surface from hydraulically fractured oil and gas wells in multiple basins. We identified degradation pathways and kinetics for PEGs and PPGs under conditions simulating a spill of produced water to shallow groundwater. Sediment-groundwater microcosm experiments were conducted using four produced water samples from two Denver-Julesburg Basin wells at early and late production. High-resolution mass spectrometry was used to identify the formation of mono- and di-carboxylated PEGs and mono-carboxylated PPGs, which are products of PEG and PPG biodegradation, respectively. Under oxic conditions, first-order half-lives were more rapid for PEGs (<0.4–1.1 d) compared to PPGs (2.5–14 d). PEG and PPG degradation corresponded to increased relative abundance of primary alcohol dehydrogenase genes predicted from metagenome analysis of the 16S rRNA gene. Further degradation was not observed under anoxic conditions. Our results provide insight into the differences between the degradation rates and pathways of PEGs and PPGs, which may be utilized to better characterize shallow groundwater contamination following a release of produced water.

Received 30th June 2018 Accepted 8th September 2018

DOI: 10.1039/c8em00291f

rsc.li/espi

#### **Environmental significance**

Given the frequency of surface spills of produced fluids from unconventional oil and gas operations, there is a need to better characterize the resulting groundwater contamination. Produced fluids are known to have complex and variable chemical and microbial composition that could influence contaminant fate and transport in groundwater; however, studies on the behavior of compounds measured in produced water under environmentally relevant conditions are limited. This study investigates the degradation pathways and kinetics of the frequently used ethoxylated surfactants polyethylene glycol and polypropylene glycol under conditions simulating a release to shallow groundwater of produced water from two hydraulically fractured oil and gas wells at varying production times. These results may be utilized to better characterize shallow groundwater contamination following a release of produced water.

#### Introduction

The combined technologies of horizontal drilling and hydraulic fracturing have facilitated rapid expansion of unconventional oil and gas development, raising a number of public concerns including the introduction of chemicals used in hydraulic fracturing fluids into the environment.<sup>1-3</sup> Hydraulic fracturing fluids are pumped into low-permeability hydrocarbon-bearing formations at high pressures to enhance well production. A typical fracturing fluid is composed of about 90% water, 9% sand, and 0.5–3% chemical additives.<sup>4-6</sup> Following well stimulation, fracturing fluids along with formation brines are coproduced with hydrocarbons, referenced herein as "produced water." Recent studies and advances in analytical methods have improved the knowledge of the composition of produced water,<sup>7-9</sup> which has been shown to vary between different wells, formations, and production ages.<sup>8-11</sup>

Several studies have reported groundwater contamination linked to known or suspected releases of oil- and gas-related fluids. <sup>12-14</sup> In the Denver-Julesburg Basin in northeastern

<sup>&</sup>lt;sup>a</sup>Department of Civil, Environmental and Architectural Engineering, University of Colorado Boulder, 607 UCB, Boulder, CO 80309, USA. E-mail: joseph.ryan@colorado.edu

<sup>&</sup>lt;sup>b</sup>S.S. Papadopulos & Associates, Inc., Boulder, CO 80303, USA

Department of Civil, Environmental and Geodetic Engineering, The Ohio State University, Columbus, OH 43210, USA

<sup>&</sup>lt;sup>d</sup>Department of Civil and Environmental Engineering, University of New Hampshire, Durham, NH 03824, USA

<sup>†</sup> Electronic supplementary information (ESI) available: Additional details on methods; MS-MS for PEG-diCOOH and PPG-COOH products; 10 tables and 16 figures detailing compound identification, redox and ATP results, and microbial community analysis. See DOI: 10.1039/c8em00291f

Colorado, the number of reported surface spills that contaminated shallow groundwater with one or more of benzene, toluene, ethylbenzene, and xylenes increased from about 60 to 100 spills annually between 2007 and 2014. <sup>15</sup> Produced water has been reported as one of the most frequently released materials in most major United States unconventional resource plays. <sup>16,17</sup> Given the frequency of accidental surface spills, there is a need to understand the natural attenuation rates and pathways of organic constituents identified in the produced fluids.

Homologous series of polyethylene glycols (PEG) and polypropylene glycols (PPG) have been detected in produced water from multiple basins. PEGs and PPGs are frequently reported as constituents in fracturing fluid additives including surfactants, emulsifiers, and crosslinkers. A recent study of the temporal evolution of produced water composition in the Denver-Julesburg Basin showed that PEGs and PPGs were present after 400 days of production. PEGs and PPGs have been suggested as potential environmental tracers because they have been frequently reported in produced water and are present from the injected fluids as opposed to being natural constituents of the formation brines. 11,19

Recent studies have shown biodegradation to be an important removal mechanism for some organic compounds identified in fracturing fluids and produced water under environmentally relevant conditions.24-28 PEGs have been reported to rapidly biodegrade under aerobic conditions.<sup>28-31</sup> While PPGs have also been found to be biodegradable under aerobic conditions, 29,31-33 they have been shown to be more persistent than PEGs.<sup>29,31</sup> Under aerobic conditions, both PEGs and PPGs are biotransformed through stepwise shortening of terminal primary alcohol groups via alcohol and aldehyde dehydrogenase enzymatic pathways in succession, producing carboxylated intermediates.34,35 Anaerobically, PEGs are biodegraded via the diol dehydratase pathway,36 while PPGs have been shown to be more recalcitrant under anoxic conditions.36-38 Given their relatively hydrophilic nature, PEGs and PPGs are expected to be fairly mobile in groundwater.

Our objective was to measure degradation pathways and kinetics for PEGs and PPGs under conditions simulating a release of produced water into shallow groundwater. Produced water chemical and microbiological composition varies between different wells and production ages; 10,11 thus, sediment-groundwater microcosm experiments were conducted using four produced water samples from two Denver-Julesburg Basin wells at early and late production. High resolution mass spectrometry was complemented by analysis of microbial community dynamics and predictive metagenomics analysis to investigate PEG and PPG degradation pathways and kinetics.

#### **Methods**

#### **Produced water samples**

Four produced water samples were collected from two horizontal wells (referenced as wells "A" and "B") targeting the Niobrara Formation in the Denver-Julesburg Basin in Weld County, Colorado. Both wells were hydraulically fractured with gel-based treatments (Tables S1 and S2†). Samples were

collected from each well at early and late production times. Early time samples were collected 22 d after production began from well A ("A-22") and 14 d after production began from well B ("B-14"). Late time samples were collected 611 d after production began from well A ("A-611") and 161 d after production began from well B ("B-161"). All samples were collected from the gas/oil/water separator in pre-baked 4 L amber glass jugs with no headspace, and stored at 4  $^{\circ}$ C.

#### Aquifer material and groundwater composition

Sediments were collected via a hand auger between the depths of 0.9 m (depth of the water table) and 2.5 m from an alluvial aquifer adjacent to the South Platte River in the Denver-Julesburg Basin. The formation is characterized as unconsolidated, coarse-grain sand and gravel with interbedded clays in some areas. <sup>39</sup> Collected sediments were homogenized, sieved through a 2 mm mesh, and stored saturated with native groundwater at 4  $^{\circ}$ C (details in the ESI†). Sieved sediments were composed of well-graded sand, with an organic carbon content of 0.37% w/w (Table S3†).

During a release, spilled fluids mix with shallow groundwater; thus, the produced water was diluted with a synthetic groundwater representative of Denver-Julesburg Basin surficial aquifers with respect to major ions and pH (details in the ESI†). The synthetic groundwater was dominated by sodium and sulfate with a pH of 7.5 (Table S3†). Dilution factors ranged from  $7-12\times$  and were determined by normalizing the initial benzene concentration in the microcosms to 1 mg L<sup>-1</sup>, which was representative of groundwater concentrations measured immediately following surface spills of produced water in the Denver-Julesburg Basin (details on spill analysis are provided in the ESI†).

#### Microcosm experiments

Microcosm experiments were conducted using sacrificial sampling. Individual microcosms were constructed by diluting the produced water with synthetic groundwater (7–12×) and adding 100 mL of the mixture to 125 mL pre-baked borosilicate glass serum bottles with 25 g of saturated sediments (1 : 5 solids-to-liquids ratio). Abiotic control microcosms were prepared for each produced water sample by adding 5.0 g L $^{-1}$  sodium azide to the synthetic groundwater (NaN $_3$ ,  $\geq$ 99%, Amresco). For each produced water treatment, triplicates (biotic) or duplicates (abiotic controls) were sacrificed at every time point. The serum bottles were sealed with PTFE-lined septa with a 10% v/v regular atmosphere headspace, which allowed the microcosms to progress from initially oxic to more reducing conditions. Bottles were mixed continuously on an orbital shaker (100 rpm) in the dark at 21  $\pm$  1  $^{\circ}$ C.

Microcosm samples were collected using sterile needles and glass syringes. Dissolved oxygen (DO) and pH were measured immediately using a luminescent dissolved oxygen probe (LDO101, Hach) and a pH electrode (PHC301, Hach). DO was considered depleted at 1.5 mg  $\rm L^{-1}$  due to the sampling procedure; it was not possible to eliminate all opportunities for reoxygenation of the sample. Samples for the analysis of major anions and cations were syringe-filtered (0.2  $\mu m$ ,

polyethersulfone membrane, Pall Corporation). Cation samples were preserved with 1% nitric acid and analyzed using inductively coupled plasma-optical emission spectroscopy (model 3410+, Applied Research Laboratories). Anions were analyzed by ion chromatography (model 4500I, Dionex). Suspended and attached adenosine triphosphate (ATP) was measured using a luminescence assay and luminometer (PhotonMaster, LuminUltra). Method details for ion and ATP analysis are provided in the ESI.† Total dissolved solids (TDS) were analyzed using Standard Method 2540C.40 Samples collected for PEG and PPG analysis were filtered through surfactant-free syringe filters18 (0.2 μm, PTFE membrane, Pall Corporation) and stored at 4 °C in 2 mL amber glass vials. Sediment samples from a subset of the A-22 and A-611 (d 0, 1, 3, 21, 49, and 86) and B-14 (d 0, 1, 4, 20, 47, and 90) microcosms in addition to samples of the aguifer sediments prior to exposure to the produced water were collected and stored in 15 mL sterile, RNase- and DNase-free centrifuge tubes at -80 °C for microbial community analysis.

#### PEG and PPG identification and analysis

Identification of PEGs, PPGs, and degradation products was conducted by accurate mass analysis using ultra highperformance liquid chromatography quadrupole time-of-flight mass spectrometry (UHPLC/qTOF-MS).19 Analytes were separated using an UHPLC system (Series 1290, Agilent Technologies) equipped with a reversed-phase C<sub>8</sub> analytical column (150 mm × 4.6 mm, 3.5 µm particle size; Zorbax Eclipse XDB-C8, Agilent Technologies), a sample volume of 20 µL, and mobile phases A and B of 0.1% formic acid in water and acetonitrile, respectively, at a flow rate of 0.6 mL min<sup>-1</sup>. The initial mobile phase composition (10% B) was held constant for 5 min, followed by a linear gradient to 100% B after 30 min. A 10 min post-run time was used after each analysis. The UHPLC system was connected to a qTOF-MS (Model 6545, Agilent Technologies) operating in positive ion mode. Accurate mass spectra were recorded across 50-1000 m/z at 2 GHz in full-spectrum mode, and data were processed with MassHunter software. MS-MS was used to identify selected compounds (isolation width of  $\sim$ 4 m/z and collision energies of 10, 20, and 40 eV). Analytical standards are only available for mixtures of PEG and PPG homologous and not individual compounds, and ionization efficiencies may not be the same for all homologues.8,11 Thus, concentrations in day 0 microcosm samples were estimated from 1 mg L<sup>-1</sup> PEG-400 and PPG-425 standards (polydispersal mixtures of PEGs and PPGs with average molecular weights of 400 and 425, respectively; Sigma-Aldrich), using the total response of all homologues. PEGs, PPGs, and identified products were semiquantified by comparing the integrated response of each homologue detected in the microcosm samples to the corresponding homologues measured in the day 0 microcosm sample.

Following the identification of PEGs, PPGs, and products by accurate mass analysis, high-performance liquid chromatography mass spectrometry (HPLC/MS) was used to semi-quantify PEG and PPG concentrations to estimate removal kinetics. Analytes were separated at 25 °C using an HPLC system (Series 1100, Agilent Technologies) equipped with an analytical column

as described above. The mobile phase composition was identical to the UHPLC/qTOF-MS method with a flow rate of 0.4 mL min<sup>-1</sup> and an increased sample injection volume of 40 µL. The HPLC system was connected to an ion trap MS (LC-MSD Trap XCT Plus, Agilent Technologies) using electrospray ionization (ESI) operating in full-scan, positive ion mode (m/z scan range 50–1000). Pseudo-first-order removal rate coefficients were estimated by linear regression using OriginPro 2016 for the period of observed rapid removal (e.g., within the linear range).

#### DNA extraction, sequencing, and bioinformatics analysis

Total nucleic acids were extracted in replicate from 0.25 g of homogenized sediment slurry using the DNeasy PowerSoil Kit (Qiagen). Triplicate replicates were extracted for all A-22, A-611, and B-14 microcosm sediment samples except day 0 (extracted in singlet) and aquifer sediment samples (extracted in duplicate). Sediment samples from the B-161 microcosms were not analyzed for microbial community analysis. DNA was quantified and quality checked using a NanoDrop 2000 (Thermo Fisher Scientific), and the polymerase chain reaction (PCR) amplification of the appropriately sized template was checked prior to sequencing. Library preparation and amplification of the V4 region of the 16S rRNA gene was performed at the Argonne National Lab according to a previously established protocol41 using primers 515F-806R. The 16S rRNA iTag sequence data were obtained by using an Illumina MiSeq at the Argonne National Lab. Sequences were processed using the QIIME 1.9.1 pipeline and Ohio Supercomputer 42,43 using closed reference operational taxonomic unit (OTU) picking against the GreenGenes database (v.13.8)44 with BLASTn and QIIME parameters set at 97% similarity.42 An OTU table was generated using taxonomic assignments from BLAST45 for all statistical analyses. Rarefaction curves were generated to evaluate the sequencing depth (Fig. S1 and S2†) and alpha diversity indices were generated in QIIME. After the removal of singlets, the OTU table was submitted to the Galaxy portal of the Langille Lab (v.1.1.1) for PICRUSt analysis for predictive metagenome analysis from the 16S rRNA gene.46 The gene abundances of primary alcohol dehydrogenase genes (PA-DH, KEGG Orthology identifier K00114)<sup>47</sup> and anaerobic diol dehydratase genes (pduC, K01699)36 were normalized to copies of a housekeeping gene, recA (K03553), to account for fluctuations in the number of predicted metagenomes through time and genomes present but lacking functional genes of interest (Fig. S3†).36,48 PICRUSt has been shown to yield accurate predictions based on small numbers of 16S rRNA gene sequences across a breadth of environmental systems.46 Statistical testing was performed using R (v.3.4.3). The 16S rRNA gene sequences were submitted to the NCBI database and are available under BioProject ID PRJNA445449.

#### Results and discussion

#### Microcosm water chemistry

The microcosms were initially oxic and progressed to more reducing conditions. The oxic/anoxic transition was rapid for the A-22 and B-14 microcosms (3 and 4 d, respectively), and

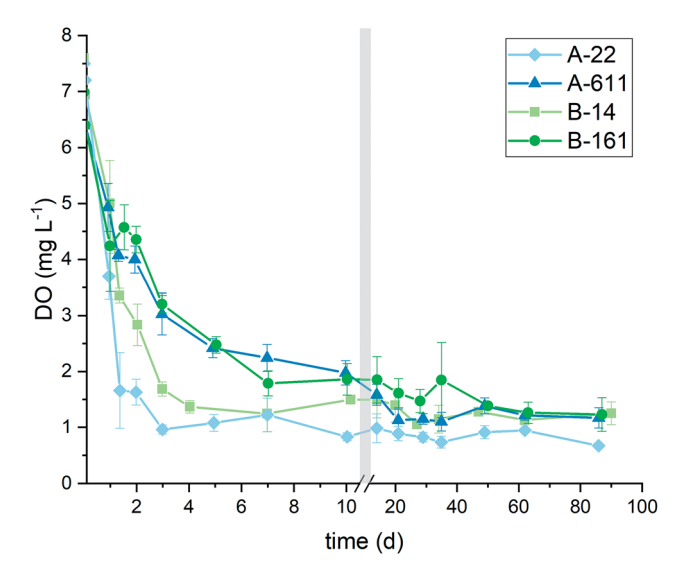


Fig. 1 Dissolved oxygen (DO) vs. time in the A-22 (diamond symbols), A-611 (triangles), B-14 (squares), and B-161 (circles) microcosm experiments.

slower for the A-611 and B-161 microcosms (21 and 28 d, respectively; Fig. 1). In all biologically active microcosms, oxygen and nitrate were simultaneously depleted; thus, the oxic period consisted of mixed oxygen- and nitrate-reducing conditions (Fig. S4-S7†). Following the oxic/anoxic transition, the different microcosms progressed to more reducing conditions, with final conditions ranging from mixed manganese- and ironreducing (A-611 and B-161 microcosms) to sulfate-reducing (A-22 and B-14). In the abiotic control microcosms, dissolved oxygen remained approximately saturated throughout the experiment, and no significant changes were observed in the concentrations of any redox-active species (Fig. S4-S7†). TDS concentrations in the microcosms were relatively low (1920-3260 mg  $L^{-1}$ , Table S7†). In all microcosms, the pH quickly dropped from approximately 7.5 to 7.0, and subsequently remained steady throughout the experiment (Fig. S8†).

In all biotic microcosms, ATP production rapidly increased during the oxic period (Fig. S9†). Under oxic conditions, a sharp increase to 10¹¹¹ to 10¹¹¹ pg total ATP (suspended and attached) occurred within the first 2 d for all water samples. Following the oxic/anoxic transition, total ATP in the A-22 and B-14 microcosms rapidly declined by two orders of magnitude, after which ATP concentrations remained steady throughout the remainder of the experiment. In both the A-611 and B-161 microcosms, the initial ATP peak was followed by a steady decline to approximately 10² pg total ATP. For all produced water treatments, ATP concentrations in the abiotic control microcosms were at least two orders of magnitude lower than those in the corresponding biotic microcosms. Rapid ATP production which corresponded to distinct redox transitions indicate significant microbial activity in the biotic microcosms.

#### Identification and transformation products

Polyethylene glycols (PEGs). PEGs were identified by accurate mass analysis. The average measured mass difference

between PEG homologues was 44.0262 u, which represents the addition of one ethylene oxide unit (-CH<sub>2</sub>CH<sub>2</sub>-O-).<sup>19</sup> Series of PEG homologues with three to fourteen ethylene oxide units were detected in all four produced water samples (Fig. 2; Table S8†).

The relative abundance of shorter chain PEGs was greater in the initial distribution of the PEG series detected in the A-22 day 0 microcosm relative to the B-14 day 0 microcosm (Fig. 2a and c). The initial distribution of PEGs was nearly identical in A-22 and A-611 (Fig. 2a and b); however, there was a shift towards shorter chains in B-161 compared to B-14 (Fig. 2c and d). The estimated total concentration of all PEG homologues in the A-22 day 0 microcosm was in the mg L<sup>-1</sup> range and was approximately an order of magnitude greater than that of the B-14 day 0 microcosm. Differences in the initial PEG distributions and concentrations between the two wells were likely due to varying fracturing fluid composition. The FracFocus Chemical Disclosure Registry49 report for well A listed PEGs as an ingredient. Well B's FracFocus report listed a proprietary "surfactant blend" and did not specifically report the use of PEGs (Tables S1 and S2†). Downhole reactions could explain the distribution differences between the two production ages in well B. Based on hydrophobicity, sorption to the hydrocarbon formation would not be a significant downhole removal mechanism for the relatively short-chained PEGs returning to the surface.18 ATP concentrations indicated biological activity in the produced water collected from B-14 (8010 pg L<sup>-1</sup> suspended ATP), while ATP concentrations were approximately 3 orders of magnitude lower in the A-22 produced water sample (10 pg L<sup>-1</sup> suspended ATP). Thus, downhole biodegradation could have occurred in well B, but low biomass activity suggests that downhole biodegradation was unlikely in well A. Shifts to smaller homologues have been reported during PEG biodegradation, 29,30 which could explain the distribution differences between B-14 and B-161.

After day 1 of the microcosm experiment, chromatographic peaks separated by 44.0262 u (one ethylene oxide group) were observed eluting approximately 0.5 min later than the detected PEGs (Fig. 3). The peak at 11.4 min had a measured mass of 460.2396 with companion adducts at m/z 465.1947 and 443.2126 (Fig. S10†). Based on mass differences, the ions were identified as the ammonium, sodium, and proton adducts, respectively. Fig. S10† also shows ions at m/z 487.1764 and 509.1582, which are 21.9815 and 43.9635 greater than the single sodium adduct, respectively. The mass difference equates to the addition of a sodium ion minus a proton, indicating the presence of double (m/z 487.1764) and triple (m/z 509.1582) sodium adducts. Accurate mass putatively identified a formula of C<sub>18</sub>H<sub>34</sub>O<sub>12</sub>Na<sup>+</sup> (single sodium adduct) with a calculated exact mass of m/z465.1942, which is within 1.1 ppm of the measured mass. The compound was putatively identified as a di-carboxylated PEG (PEG-diCOOH). The double and triple sodium adducts occur when one or both carboxyl groups, respectively, are in the form of a sodium salt. MS-MS was conducted (details in S2.1; Fig. S11†). The ions formed were consistent with the structure of the putative PEG-diCOOH; however, a standard was not available and thus prevented final confirmation. Mono-

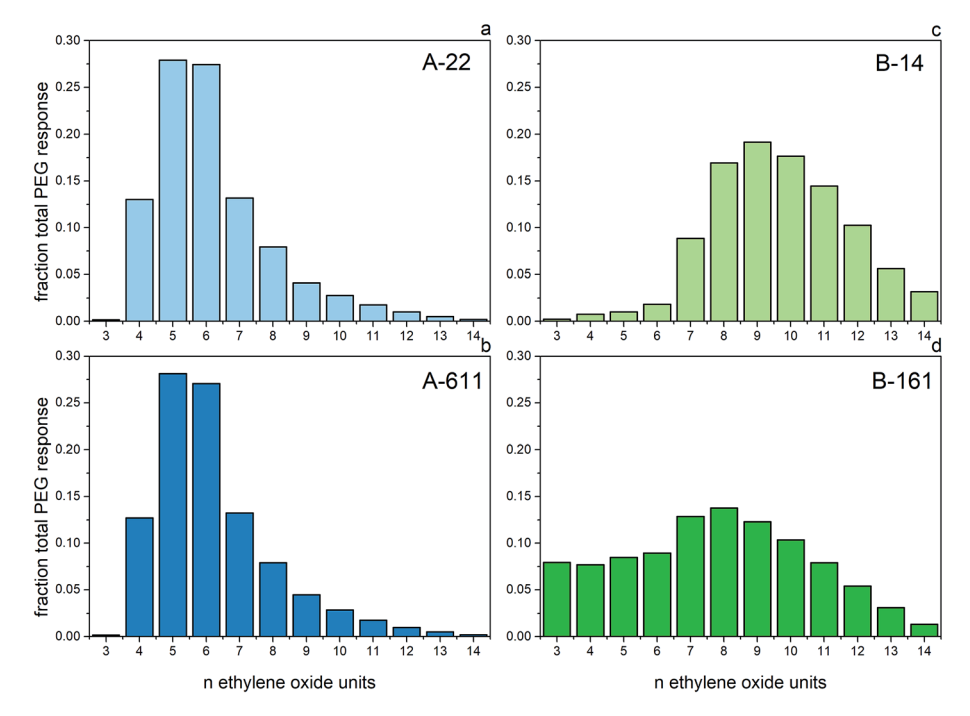


Fig. 2 Initial (day 0) distribution of PEG homologues in (a) A-22, (b) A-611, (c) B-14, and (d) B-161 microcosms.

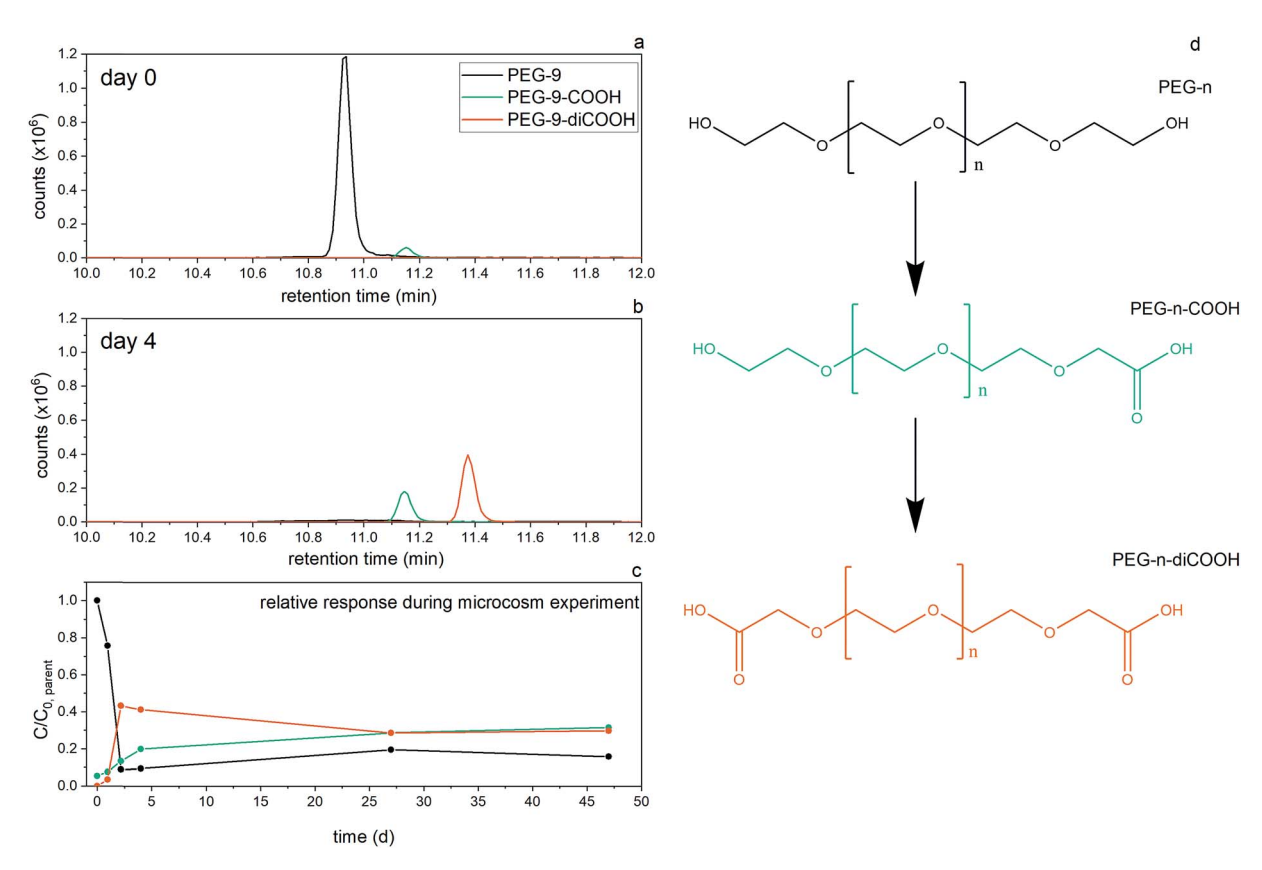


Fig. 3 Chromatographic separation of PEG-9 (black trace) and corresponding products PEG-9-COOH (green trace) and PEG-9-diCOOH (orange trace) on (a) day 0 and (b) day 4 of the B-14 microcosm experiment, and (c) response (integrated peak area) of the three compounds relative to PEG-9 ( $C/C_{0,parent}$ ) during the microcosm experiment. The aerobic metabolic pathway is shown (d).

carboxylated PEGs (PEG-COOH) were also identified by accurate mass analysis (e.g., peak at 11.1 min apparent in Fig. 3b). Single carboxylated PEGs have been previously reported in produced water.19 The small increase in retention time for the carboxylated products (Fig. 3b) can be explained by the slightly greater hydrophobicity of protonated PEG-COOH and PEGdiCOOH compared to the parent PEG in the acidic mobile phase in addition to increasing molecular weights (+14 u) of the carboxylated products. Thurman et al. 18,19 demonstrated via the Kendrick mass scale that for homologous series of ethoxylates it is only necessary to identify the structure of one homologue in the series, and that the remaining compounds represent the addition of ethylene oxide units. Thus, accurate-mass analysis presented for the di-carboxylated product of example homologue PEG-9 (Fig. S10†) and the MS-MS analysis conducted for the example homologue PEG-6-diCOOH (e.g., Fig. S11†) apply to the identification of all PEG homologues in the series. Both PEG-COOH and PEG-diCOOH with four to fourteen ethylene oxide units were detected in all of the microcosms (Table S8†).

PEG-COOH was detected in the day 0 microcosm samples with an integrated response that was 4–22% of the corresponding PEG; however, PEG-diCOOH was not observed until after day 1 of the microcosm experiments (Fig. 3c). Both compounds are known PEG biodegradation intermediates under aerobic conditions.<sup>34</sup> In the presence of oxygen, PEGs are enzymatically altered through oxidation of the terminal primary alcohol group (Fig. 3d), followed by cleavage of the terminal ether bonds to produce a shorter-chained PEG with two fewer ethylene oxide units.<sup>34,35</sup> The detection of PEG-COOH in the day 0 microcosm samples suggests that it may be present initially as an impurity in the industrial surfactant mixture used in the fracturing fluid.<sup>19</sup> Downhole degradation is unlikely because

only the PEG-COOH and not the PEG-diCOOH was detected in the day 0 microcosm samples. Nevertheless, the increasing response of PEG-COOH with time and the emergence of PEG-diCOOH (not present on day 0) in conjunction with the removal of the corresponding PEG provides strong evidence of further formation of the carboxylated products in the microcosms (Fig. 3). Mass spectrometry analysis was not conducted for abiotic control samples due to high sodium azide concentrations used to inhibit microbial activity; thus, information needed to distinguish abiotic and biotic removal mechanisms was not obtained. Significant abiotic removal of PEGs has not been reported;<sup>28</sup> therefore, PEG transformation and removal observed in the microcosms was almost surely a result of biodegradation.

**Polypropylene glycols (PPGs).** PPGs were also identified by accurate mass analysis. The average measured mass difference between PPG homologues was 58.0419 u, which represents the addition of one propylene oxide unit (-CH<sub>2</sub>CH(CH<sub>3</sub>)-O-).<sup>19</sup> Series of PPG homologues ranging from two to ten propylene oxide units were detected in all four produced water samples (Fig. 4; Table S9†).

There was a greater relative abundance of shorter chain PPGs in the initial distribution of the PPG series present in the A-22 day 0 microcosm compared to the B-14 day 0 microcosm (Fig. 4a and c). The initial PPG distribution was shifted towards shorter chains in the A-611 and B-161 microcosms (Fig. 4b and d) compared to A-22 and B-14, respectively. The estimated total PPG concentration was in the range of hundreds of  $\mu g \; L^{-1}$  and was approximately an order of magnitude lower in the A-22 day 0 microcosm compared to B-14. The differences in the initial PPG distributions and concentrations between the two wells and production times could be due to both varying fracturing

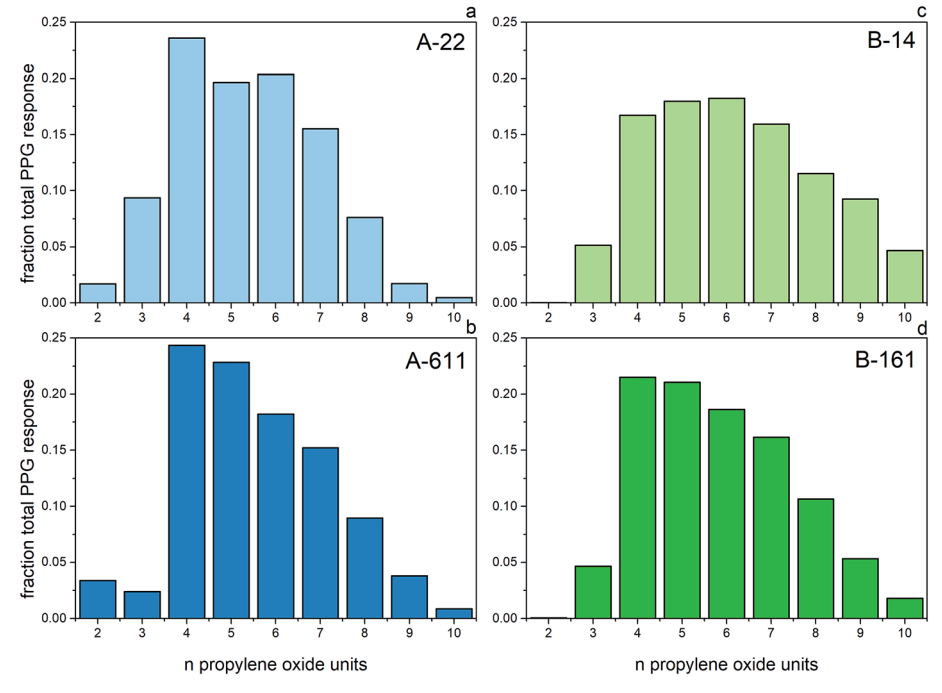


Fig. 4 Initial (day 0) distribution of PPG homologues in (a) A-22, (b) A-611, (c) B-14, and (d) B-161 microcosms.

fluid composition and downhole reactions including shale interactions. FracFocus reports from both wells cited proprietary "surfactant blends," but PPGs or blends of ethoxylated surfactants were not specifically identified in either report. PPGs are more hydrophobic than PEGs;11 thus, sorption of longer-chained PPGs to the hydrocarbon formation or partitioning to the oil phase could contribute to the shift towards shorter-chained homologues observed at later production times. Sorption of longer-chained PPGs could explain the similar initial distributions observed in both the A-611 and B-161 day 0 microcosms.

After day 1 of the microcosm experiment, chromatographic peaks separated by 58.0419 u (one propylene oxide group) were observed approximately 0.2 min after the detected PPGs. With the same approach used to identify PEG-diCOOH, sodium (m/z)403.2302), proton (m/z 381.2483), and ammonium (m/z398.2749) adducts were measured for the peak from 16.0-16.6 min (Fig. S12†). Accurate mass putatively identified a formula of C<sub>18</sub>H<sub>36</sub>O<sub>8</sub>Na<sup>+</sup> (sodium adduct) with a calculated exact mass of m/z 403.2302, which was an exact match to the measured mass. The compound was putatively identified as a mono-carboxylated PPG (PPG-COOH). Analogous to the PEG carboxylates, a double sodium adduct indicated that the sodium salt of the carboxyl group was present, albeit at trace levels (m/z 425.2129; Fig. S12†). MS-MS was conducted using PPG-7-COOH as an example homologue (details in S2.2; Fig. S13†). The chromatograph of PPG-4 is shown in Fig. 5 because numerous isomers are discernable for relatively shortchained PPGs (see discussion below). PPG-COOH products with three to ten propylene oxide units were identified (Table S9†).

PPG-COOH was not detected in the day 0 microcosms (Fig. 5). A similar aerobic metabolic pathway to PEGs has been reported for PPGs: oxidation of a terminal alcohol (Fig. 5d) followed by cleavage of the terminal ether bond to produce PPGs with one fewer propylene oxide unit.32-34 The emergence of PPG-COOH corresponding to the removal of PPGs demonstrates that PPG-COOH was formed in the microcosms (Fig. 5). Significant abiotic removal of PPGs has not been reported;<sup>33,36</sup> thus, the transformation and removal observed in the microcosms was likely a result of biodegradation.

Multiple isomers were apparent for the PPG-COOH product. The number of isomers in the parent PPG increases exponentially for each additional propylene oxide unit due to nonsymmetric hydroxyl groups on the monomer. 19,33 For shortchained PPGs, individual isomers are apparent in the chromatography as distinct peaks with varying intensities. For instance, at least nine PPG-4 isomers can be discerned within the four readily apparent peaks, and at least five isomers were observed for the corresponding PPG-4-COOH (Fig. 5b). The PPG-4-COOH isomer peaks had slightly different relative intensities compared to PPG-4, which indicates that different isomers were transformed to varying extents. Variable transformation for PPG isomers has been previously suggested.33,34

In contrast to PEGs, only a singly carboxylated PPG product was identified. This is likely caused by the presence of both primary and secondary terminal alcohols in PPG isomers

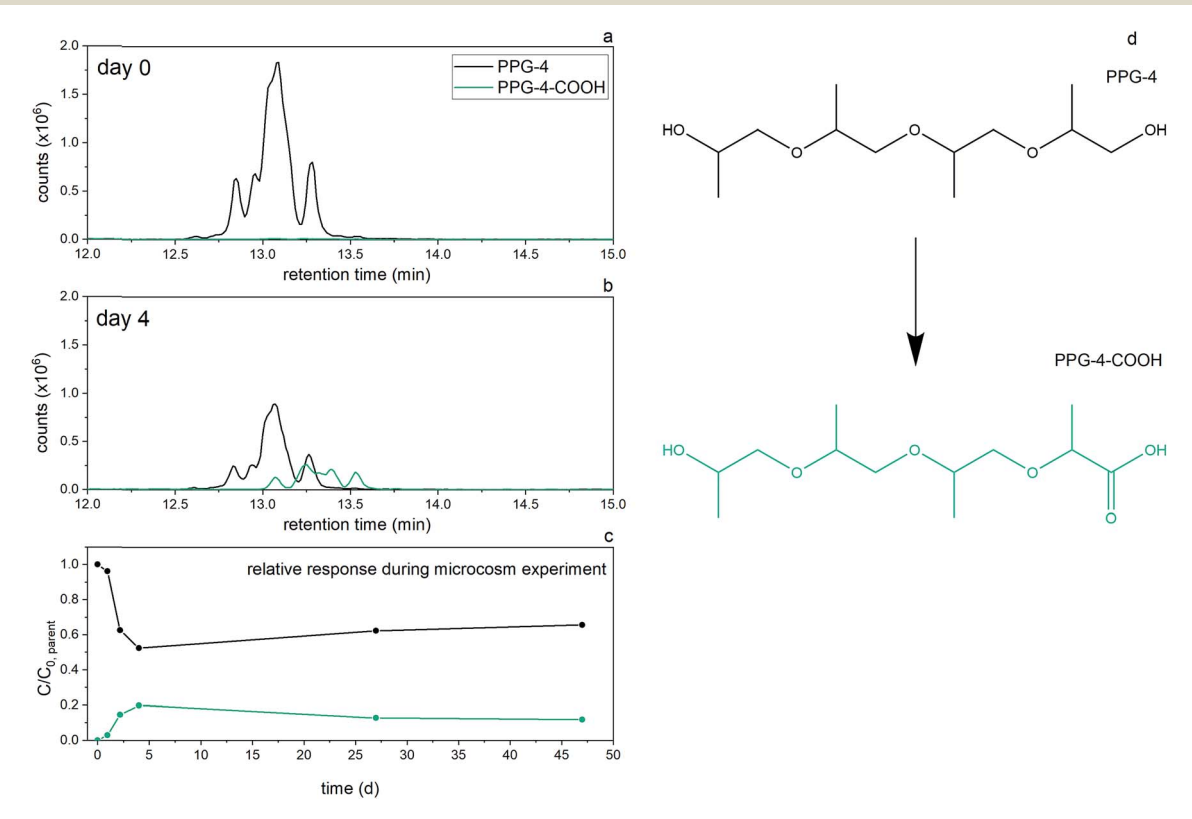


Fig. 5 Chromatographic separation of PPG-4 (black trace) and corresponding product PPG-4-COOH (green trace) on (a) day 0 and (b) day 4 of the B-14 microcosm experiment, and (c) response (integrated peak area) of the three compounds relative to PPG-4 ( $C/C_{0,parent}$ ) during the microcosm experiment. The aerobic metabolic pathway is shown (d).

resulting from the non-symmetric monomer. PEGs are symmetric homopolymers with two terminal primary alcohol groups, both of which can be oxidized to form PEG-diCOOH. For PPGs, oxidation of the terminal secondary alcohol to a carboxyl is not expected.<sup>50</sup> Thus, only PPG isomers with a terminal primary hydroxyl can be degraded to PPG-COOH. The formation of a ketone product from the terminal secondary hydroxyl has been reported;32 however, we did not observe a PPG-ketone product in our microcosm experiments.

#### **Degradation kinetics**

Semi-quantitative analysis of PEG and PPG degradation was conducted using the HPLC/MS method. PEG-9 and PPG-6 were selected as example PEG and PPG homologues, respectively, based on their relative abundance in the microcosms (Fig. 2

and 4). Fig. 6 shows the relative response of PEG-9 and PPG-6 during the microcosm experiments, including both the oxic (filled symbols) and anoxic (open symbols) periods.

Under mixed oxygen- and nitrate-reducing conditions, PEG-9 was rapidly removed in all microcosms (Fig. 6a). First-order half-lives were similar for the four microcosms (Table 1). In the A-22 and B-14 microcosms, the half-lives were 0.4 and 1.1 d, respectively. In the A-611 and B-161 microcosms, PEG-9 was not detected in the day 1.5 sample; thus, the half-life was reported as < 0.4 d. Under oxic conditions, PPG-6 degradation was faster for water collected at late production times ( $t_{1/2} = 2.7$  and 2.5 d in A-611 and B-161 microcosms, respectively) compared to early production times ( $t_{1/2} = 7.5$  and 14 d in A-22 and B-14 microcosms; Table 1, Fig. 6b). Our measured rates were consistent with PEG and PPG biodegradation rates reported under oxic conditions for similar initial concentrations and average

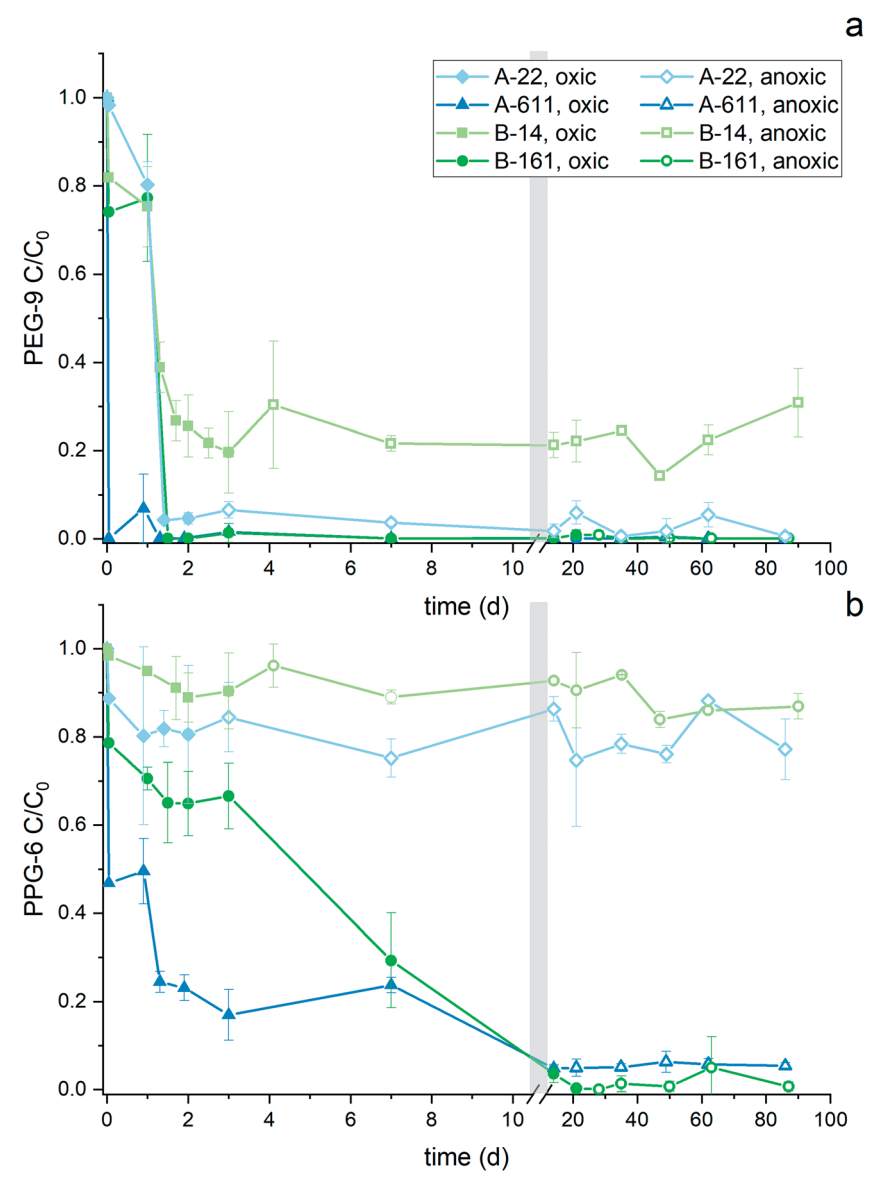


Fig. 6 Degradation of (a) PEG-9 and (b) PPG-6 in A-22 (diamond symbols), A-611 (triangles), B-14 (squares), and B-161 (circles) microcosms. Oxic and anoxic periods are represented by solid and open symbols, respectively. An axis break on day 10 is used to show details for rapid degradation.

**Table 1** Pseudo-first-order half-lives  $(t_{1/2})$  and standard error fit during the oxic period of the produced water microcosm experiments

Microcosm	PEG-9 t <sub>1/2</sub> (d)	PPG-6 t <sub>1/2</sub> (d)
A-22	$0.4\pm0.1$	$7.5 \pm 5.2$
A-611	<0.4	$2.7\pm0.5$
B-14	$1.1\pm0.2$	$14\pm3.7$
B-161	<0.4	$2.5\pm0.2$

molecular weights, by inoculum sources ranging from river water<sup>29</sup> to activated sludge.<sup>30-32</sup> Notably, the produced water mixture did not significantly inhibit or enhance PEG and PPG biodegradation compared to studies where these compounds were the only substrate. Biodegradation inhibition in mixtures of fracturing fluid organic constituents at high concentrations representative of the injected fluids has been previously reported.26,28

Under oxic conditions, PPG degradation was both slower and more variable compared to the degradation of PEGs (Fig. 6). While the occurrence of PEG-diCOOH demonstrates that PEGs can be degraded from both sides of the molecule, the monocarboxylated PPG was the only PPG product identified in the microcosms. Thus, PPGs were only degraded where a terminal primary hydroxyl was present and degradation was effectively blocked for isomers with terminal secondary hydroxyls. This likely contributed to slower degradation kinetics of PPGs compared to that of PEGs. Differences in the initial PPG concentrations may have contributed to the variable PPG degradation kinetics observed between microcosms because B-14 had both the highest estimated initial PPG concentration and the slowest degradation. A recent study under anoxic conditions suggested a concentration inhibitory effect on PPG biodegradation kinetics.36 In our study, PPG-6 degradation was overall slower than PEG-9 degradation, but the relative succession of half-lives for the different microcosms was the same for both compounds (B-14 > A-22 > A-611  $\approx$  B-161), which suggests that produced water composition also may have influenced degradation kinetics. Similar ATP concentrations in all microcosms during the period corresponding to PEG and PPG oxic degradation (1010 to 1011 pg total ATP, Fig. S9†) suggest comparable levels of overall biomass activity, and that a nonspecific inhibitor such as a biocide likely did not affect the degradation kinetics. Competitive inhibition from a more labile or preferred carbon source present in the early-time produced water could have slowed the rate of PEG and PPG degradation relative to the water from later production times. This is consistent with the rapid depletion of dissolved oxygen observed in the A-22 and B-14 microcosms compared to the A-611 and B-161 microcosms (Fig. 1), which could indicate more competition for available electron acceptors. TDS concentrations greater than 10 000 mg L<sup>-1</sup> can inhibit biological activity;<sup>7</sup> however, TDS concentrations in the microcosms were below this threshold (1920–3260 mg  ${
m L}^{-1}$ , Table S7†) and likely did not inhibit degradation.

There was no evidence of further PEG or PPG degradation under anoxic conditions. In the A-22 and B-14 microcosms, low levels of PEG-9 remained at the oxic/anoxic transition (Fig. 6a),

but no additional removal was observed. In the A-611 and B-161 microcosms, PEG-9 was not detected at the oxic/anoxic transition, likely because the longer oxic period allowed for more complete removal. Anaerobic biodegradation of PEGs has been reported at temperatures  $\geq 35 \, {}^{\circ}\text{C}$ , 51,52 so it is possible that either the anaerobic microbial community in the microcosms was unable to degrade PEGs, or the kinetics were slow enough under ambient temperatures that no degradation was observed over the 84-86 d anoxic periods. Due to both different degradation rates and lengths of the oxic period for the four microcosms, varying levels of PPG-6 remained at the oxic/anoxic transition (Fig. 6b); however, no further removal was observed under anoxic conditions in any microcosm. Our observations are in agreement with studies that have reported PPGs to be recalcitrant under anaerobic conditions, particularly in the presence of microbial communities which have not been previously exposed to glycols.36-38

#### Microbial community dynamics and abundance of primary alcohol dehydrogenase genes

Analysis of microbial community dynamics and function based on metagenomes predicted from the 16S rRNA gene provides further insight into the PEG and PPG biodegradation pathway. After quality filtering and processing, 14 640-77 563 sequences per sample were obtained (Table S10†). One triplicate sample of B-14 day 4 yielded very low sequence counts (3010) and was not used in any analysis; therefore, the error bars associated with this sample represent a range of duplicate values. Exposure to produced water greatly decreased the diversity of sediment microbial communities: Shannon's diversity index was 10 in the aquifer sediments prior to exposure to the produced water and dropped to 5-7 by day 3-4 of the microcosm experiments. Similarly, microbial community richness decreased from over 3500 OTUs in the aguifer sediments to 1300-2700 OTUs in microcosm sediment samples in 1-4 days.

Using a bioinformatics approach (PICRUSt), we searched for genes known to catalyze polyglycol chain shortening in metagenomes predicted from 16S rRNA gene sequences. While specific PEG- and PPG-degrading enzymes have been proposed,35,53 they remain poorly characterized. Thus, primary alcohol dehydrogenase genes (PA-DH) were used as a proxy for polyglycol biotransformation under oxic conditions via terminal alcohol oxidation. PA-DH is found in several taxonomic groups, including Pseudomonas, when grown on a wide variety of alcohols and acts by oxidation of terminal primary hydroxyl groups.<sup>54</sup>

A sharp increase in the abundance of the PA-DH gene relative to the housekeeping gene recA (PA-DH/recA) was observed during the first 1-3 days of the A-22, A-611, and B-14 microcosms (Fig. 7), which coincided with the period of rapid PEG and PPG removal (Fig. 6). In the A-22 and B-14 microcosms, the relative abundance of PA-DH/recA initially spiked to approximately 0.40 normalized gene copies, followed by a decrease to <0.25. The relative abundance of PA-DH/recA in the A-611 microcosms initially increased to 0.52 and remained elevated for the duration of the microcosm experiment, which is consistent with faster removal observed in the late-time

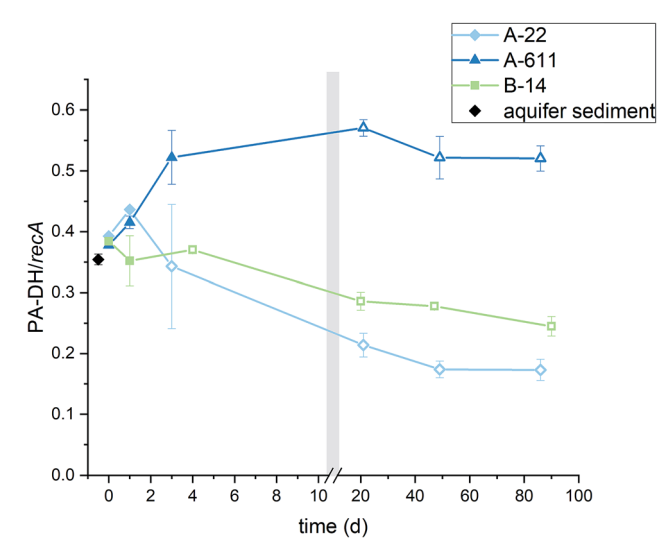


Fig. 7 Abundance of the primary alcohol dehydrogenase gene (PA-DH) relative to a housekeeping gene (recA) generated from metagenomes predicted from the 16S rRNA gene of microbial communities in the A-22 (diamond symbols), A-611 (triangles), and B-14 (squares) microcosms, in addition to the aquifer sediment prior to exposure to produced water (black diamond symbol). Oxic and anoxic periods are represented by solid and open symbols, respectively.

compared to the early-time produced water. The prolonged presence of dissolved oxygen in A-611 microcosms compared to A-22 and B-14 (Fig. 1) also may have enabled the persistence of microbial taxa capable of encoding PA-DH genes, which are repressed under reducing conditions. Trace levels of the diol dehydratase gene *pduC*, associated with polyglycol chain shortening under anaerobic conditions, <sup>36</sup> were predicted in the microcosm samples; however, *pduC* abundance was at least three orders of magnitude less than that of PA-DH, which is consistent with the limited PEG and PPG removal observed after the microcosms changed from oxic to anoxic conditions.

Pseudomonas became highly enriched in all of the microcosms over time, increasing from 0.01% of the aquifer sediment community to 50-65% by day 3 and remaining between 20 and 50% of the terminal community in microcosm sediments (Fig. S14†). Pseudomonas has been identified in produced fluids as an important member of hydraulically fractured shale communities55-57 and was enriched during biodegradation of synthetic hydraulic fracturing fluid in soil-groundwater microcosms.24 Many species of Pseudomonas have the enzymatic capacity to degrade PEGs; therefore, this taxon may contribute to PEG degradation in the microcosms. 58-61 The genus Syntrophobotulus was also detected, a taxon notable for fermenting glyoxylate,62 a proposed product of aerobic PEG chain shortening.34 Genes participating in oxic and anoxic transformations of glyoxylate were also predicted in the samples (K01638/ EC2.3.3.9 and K00015/EC1.1.1.26), suggesting that mineralization of these products may have occurred in the microcosms.

#### Implications of PEG and PPG degradation in groundwater

Collectively, the predicted presence of genes associated with enzymatic pathways for the aerobic degradation of PEGs, PPGs,

and their metabolites combined with the identification of mono- and di-carboxylated intermediate polyglycol products supports the inference that PEG and PPG removal during the oxic phase was largely due to biodegradation. These results demonstrate the role that aerobic sediment microorganisms are likely to play in degrading PEG and PPG polymers, with implications for disruption of the natural microbial community (*i.e.*, lower diversity and/or enrichment of key taxa) in the event of a release of produced water into shallow groundwater.

Given the persistence observed in our microcosms under anoxic conditions, PEGs and PPGs are more likely to be detected at sites where anoxic conditions prevail. The degradation products identified in our microcosms could help characterize the releases of produced water into shallow groundwater even when the parent compounds have been largely transformed. The PPG-COOH product was persistent under both oxic and anoxic conditions (Fig. 5c and S15†). Both carboxylated PEG products appeared to be persistent under anoxic conditions; however, PEG-COOH and PEG-diCOOH emerged and were both subsequently degraded during the longer oxic periods in the A-611 and B-161 microcosms (Fig. 3c and S16†). Thus, the PEG products may not be detected at sites with stable or prolonged oxic conditions.

Produced water composition is heterogeneous between different wells, formations, and production ages,8-11 which could result in variable detection or degradation kinetics of PEGs and PPGs. While the detection of PEGs and PPGs in the A-611 and B-161 samples demonstrates that these compounds may be present long after well stimulation, the lower concentrations require sensitive analytical methods to detect. We found that PPGs were more persistent in produced water with higher initial concentrations. We observed rapid PEG removal at the low concentrations present in the produced water microcosms; however, half-lives reported for high PEG concentrations, representative of the initial hydraulic fracturing fluid composition, were an order of magnitude longer.28 Rosenblum et al.11 showed that the concentrations of PEGs and PPGs in Denver-Julesburg Basin produced water decreased approximately 50% within the first two weeks of production. Thus, PEGs and PPGs are more likely to be detected at sites with a release shortly after production begins due to both higher initial concentrations and potentially slower degradation rates.

Given the frequency of accidental surface spills associated with unconventional oil and gas activities, there is a need to understand the natural attenuation rates and pathways of organic constituents in the produced fluids. Our results demonstrate the differences between PEG and PPG degradation rates and pathways. These insights may be utilized to better characterize shallow groundwater contamination following a release of produced water.

#### Conflicts of interest

There are no conflicts of interest to declare.

## Acknowledgements

This research is supported by the AirWaterGas Sustainability Research Network funded by the National Science Foundation (CBET-1240584) and the University of Colorado CEAE Department Doctoral Assistantship for Completion of Dissertation. P.J.M. and M.V.E. were partially supported by NSF CBET award no. 1823069. We thank Katherine Armstrong for assistance with sampling, Dr Fred Luiszer for assistance with ICP-OES and IC analysis, and Dr Jerry Zweigenbaum (Agilent Technologies) for support of our UHPLC/qTOF-MS instrumentation. We also thank our industry collaborator for proving access and assistance with produced water collection.

#### References

Paper

- 1 J. L. Adgate, B. D. Goldstein and L. M. McKenzie, Potential public health hazards, exposures and health effects from unconventional natural gas development, Environ. Sci. Technol., 2014, 48, 8307-8320.
- 2 A. Vengosh, R. B. Jackson, N. Warner, T. H. Darrah and A. Kondash, A critical review of the risks to water resources from unconventional shale gas development and hydraulic fracturing in the United States, Environ. Sci. Technol., 2014, 48, 8334-8348.
- 3 R. D. Vidic, S. L. Brantley, J. M. Vandenbossche, D. Yoxtheimer and J. D. Abad, Impact of shale gas development on regional water quality, Science, 2013, 340(6134), 1235009.
- 4 W. T. Stringfellow, J. K. Domen, M. K. Camarillo, W. L. Sandelin and S. Borglin, Physical, chemical, and biological characteristics of compounds used in hydraulic fracturing, J. Hazard. Mater., 2014, 275, 37-54.
- 5 I. Ferrer and E. M. Thurman, Chemical constituents and analytical approaches for hydraulic fracturing waters, Trends Environ. Anal. Chem., 2015, 5, 18-25.
- 6 M. Elsner and K. Hoelzer, Quantitative survey and structural classification of hydraulic fracturing chemicals reported in unconventional gas production, Environ. Sci. Technol., 2016, 50, 3290-3314.
- 7 A. Butkovskyi, H. Bruning, S. A. E. Kools, H. H. M. Rijnaarts and A. P. Van Wezel, Organic pollutants in shale gas flowback and produced waters: Identification, potential ecological impact, and implications for treatment strategies, Environ. Sci. Technol., 2017, 51, 4740-4754.
- 8 K. Oetjen, C. Danforth, M. C. McLaughlin, M. Nell, J. Blotevogel, D. E. Helbling, D. Mueller and C. P. Higgins, Emerging analytical methods for the characterization and quantification of organic contaminants in flowback and produced water, Trends Environ. Anal. Chem., 2017, 12-23.
- 9 J. L. Luek and M. Gonsior, Organic compounds in hydraulic fracturing fluids and wastewaters: A review, Water Res., 2017, 123, 536-548.
- 10 W. Orem, C. Tatu, M. Varonka, H. Lerch, A. Bates, M. Engle, L. Crosby and J. McIntosh, Organic substances in produced and formation water from unconventional natural gas extraction in coal and shale, Int. J. Coal Geol., 2014, 126, 20 - 31.
- 11 J. Rosenblum, E. M. Thurman, I. Ferrer, G. Aiken and K. G. Linden, Organic chemical characterization and mass balance of a hydraulically fractured well: From fracturing

- fluid to produced water over 405 days, Environ. Sci. Technol., 2017, 51, 14006-14015.
- 12 B. D. Drollette, K. Hoelzer, N. R. Warner, T. H. Darrah, Karatum, M. P. O'Connor, R. K. Nelson, L. A. Fernandez, C. M. Reddy, A. Vengosh, R. B. Jackson, M. Elsner and D. L. Plata, Elevated levels of diesel range organic compounds in groundwater near Marcellus gas operations are derived from surface activities, Proc. Natl. Acad. Sci. U. S. A., 2015, 112, 13184-13189.
- 13 S. A. Gross, H. J. Avens, A. M. Banducci, J. Sahmel, J. M. Panko and B. E. Tvermoes, Analysis of BTEX groundwater concentrations from surface spills associated with hydraulic fracturing operations, J. Air Waste Manage. Assoc., 2013, 63, 424-432.
- 14 G. T. Llewellyn, F. Dorman, J. L. Westland, D. Yoxtheimer, Sowers, E. Humston-Fulmer and Grieve, T. Brantley, Evaluating a groundwater supply contamination incident attributed to Marcellus Shale gas development, Proc. Natl. Acad. Sci. U. S. A., 2015, 112, 6325-6330.
- 15 K. J. Armstrong, J. D. Rogers, T. L. Burke and J. N. Ryan, Characterization of accidental spills and releases affecting groundwater in the Greater Wattenburg Area of the Denver-Julesburg Basin in northeastern Colorado, in SPE Health, Safety, Security, Environment, & Social Responsibility Conference - North America, Society of Petroleum Engineers, New Orleans, Louisiana, 18-20 April 2017.
- 16 K. O. Maloney, S. Baruch-Mordo, L. A. Patterson, J. P. Nicot, S. A. Entrekin, J. E. Fargione, J. M. Kiesecker, K. E. Konschnik, J. N. Ryan, A. M. Trainor, J. E. Saiers and H. J. Wiseman, Unconventional oil and gas spills: Materials, volumes, and risks to surface waters in four states of the US, Sci. Total Environ., 2017, 581, 369-377.
- 17 S. Burden, M. A. Cluff, L. E. DeHaven, C. Roberts, S. L. Sharkley and A. Singer, Review of State and Industry Spill Data: Characterization of Hydraulic Fracturing-Related Spills, EPA/601/R-14/001, U.S. Environmental Protection Agency Office of Research and Development, Washington, D.C., 2015.
- 18 E. M. Thurman, I. Ferrer, J. Blotevogel and T. Borch, Analysis of hydraulic fracturing flowback and produced waters using accurate mass: Identification of ethoxylated surfactants, Anal. Chem., 2014, 86, 9653-9661.
- 19 E. M. Thurman, I. Ferrer, J. Rosenblum, K. Linden and J. N. Ryan, Identification of polypropylene glycols and polyethylene glycol carboxylates in flowback and produced water from hydraulic fracturing, J. Hazard. Mater., 2017, 323, 11-17.
- 20 Y. H. He, S. L. Flynn, E. J. Folkerts, Y. F. Zhang, D. L. Ruan, D. S. Alessi, J. W. Martin and G. G. Goss, Chemical and toxicological characterizations of hydraulic fracturing flowback and produced water, Water Res., 2017, 114, 78-87.
- 21 K. Oetjen, K. E. Chan, K. Gulmark, J. H. Christensen, J. Blotevogel, T. Borch, J. R. Spear, T. Y. Cath and C. P. Higgins, Temporal characterization and statistical analysis of flowback and produced waters and their potential for reuse, Sci. Total Environ., 2018, 619-620, 654-664.

- 22 M. Nell and D. E. Helbling, Exploring matrix effects and quantifying organic additives in hydraulic fracturing associated fluids using liquid chromatography electrospray ionization mass spectrometry, *Environ. Sci.: Processes Impacts*, 2018, DOI: 10.1039/C8EM00135A.
- 23 J. D. Rogers, T. L. Burke, S. G. Osborn and J. N. Ryan, A framework for identifying organic compounds of concern in hydraulic fracturing fluids based on their mobility and persistence in groundwater, *Environ. Sci. Technol. Lett.*, 2015, 2, 158–164.
- 24 P. J. Mouser, S. Liu, M. A. Cluff, M. McHugh, J. J. Lenhart and J. D. MacRae, Redox conditions alter biodegradation rates and microbial community dynamics of hydraulic fracturing fluid organic additives in soil-groundwater microcosms, *Environ. Eng. Sci.*, 2016, 33(10), DOI: 10.1089/ ees.2016.0031.
- 25 D. Kekacs, B. D. Drollette, M. Brooker, D. L. Plata and P. J. Mouser, Aerobic biodegradation of organic compounds in hydraulic fracturing fluids, *Biodegradation*, 2015, 26, 271–287.
- 26 J. D. Rogers, I. Ferrer, S. S. Tummings, A. Bielefeldt and J. N. Ryan, Inhibition of biodegradation of hydraulic fracturing compounds by glutaraldehyde: Groundwater column and microcosm experiments, *Environ. Sci. Technol.*, 2017, 51, 10251–10261.
- 27 L. C. Strong, T. Gould, L. Kasinkas, M. J. Sadowsky, A. Aksan and L. P. Wackett, Biodegradation in waters from hydraulic fracturing: Chemistry, microbiology, and engineering, *J. Environ. Eng.*, 2014, 140(5), DOI: 10.1061/(asce)ee.1943-7870.0000792.
- 28 M. C. McLaughlin, T. Borch and J. Blotevogel, Spills of hydraulic fracturing chemicals on agricultural topsoil: Biodegradation, sorption, and co-contaminant interactions, *Environ. Sci. Technol.*, 2016, **50**, 6071–6078.
- 29 A. Zgola-Grzeskowiak, T. Grzeskowiak, J. Zembrzuska and Z. Lukaszewski, Comparison of biodegradation of poly(ethylene glycol)s and poly(propylene glycol)s, *Chemosphere*, 2006, **64**, 803–809.
- 30 M. Bernhard, J. P. Eubeler, S. Zok and T. P. Knepper, Aerobic biodegradation of polyethylene glycols of different molecular weights in wastewater and seawater, *Water Res.*, 2008, **42**, 4791–4801.
- 31 E. Beran, S. Hull and M. Steininger, The relationship between the chemical structure of poly(alkylene glycol)s and their aerobic biodegradability in an aqueous environment, *J. Polym. Environ.*, 2013, **21**, 172–180.
- 32 A. Zgola-Grzeskowiak, T. Grzeskowiak, J. Zembrzuska, M. Franska, R. Franski, T. Kozik and Z. Lukaszewski, Biodegradation of poly(propylene glycol)s under the conditions of the OECD screening test, *Chemosphere*, 2007, 67, 928–933.
- 33 R. J. West, J. W. Davis, L. H. Pottenger, M. I. Banton and C. Graham, Biodegradability relationships among propylene glycol substances in the organization for economic cooperation and development ready- and seawater biodegradability tests, *Environ. Toxicol. Chem.*, 2007, 26, 862–871.

- 34 F. Kawai, Microbial degradation of polyethers, *Appl. Microbiol. Biotechnol.*, 2002, **58**, 30–38.
- 35 J. P. Eubeler, M. Bernhard and T. P. Knepper, Environmental biodegradation of synthetic polymers II. Biodegradation of different polymer groups, *Trends Anal. Chem.*, 2010, 29, 84– 100.
- 36 K. M. Heyob, J. Blotevogel, M. Brooker, M. V. Evans, J. J. Lenhart, J. Wright, R. Lamendella, T. Borch and P. J. Mouser, Natural attenuation of nonionic surfactants used in hydraulic fracturing fluids: Degradation rates, pathways, and mechanisms, *Environ. Sci. Technol.*, 2017, 51, 13985–13994.
- 37 S. Wagener and B. Schink, Fermentative degradation of nonionic surfactants and polyethylene-glycol by enrichment cultures and by pure cultures of homoacetogenic and propionate-forming bacteria, *Appl. Environ. Microbiol.*, 1988, 54, 561–565.
- 38 D. F. Dwyer and J. M. Tiedje, Metabolism of polyethylene glycol by two anaerobic bacteria, *Desulfovibrio Desulfuricans* and a *Bacteroides sp*, *Appl. Environ. Microbiol.*, 1986, 52, 852–856.
- 39 ed. S. S. Paschke, Groundwater Availability of the Denver Basin Aquifer System, Professional Paper 1770, U.S. Geological Survey, Colorado, Reston, Va., 2011.
- 40 American Public Health Association, American Water Works Association, Water Environment Federation, *Standard Methods for the Examination of Water and Wastewater*, United Book Press, Inc., Baltimore, MD, 20th edn, 1998.
- 41 Earth Microbiome Project, 16S Illumina Amplicon Protocol, http://press.igsb.anl.gov/earthmicrobiome/protocols-and-standards/16s/, (accessed Aug 2017).
- 42 J. G. Caporaso, J. Kuczynski, J. Stombaugh, K. Bittinger, F. D. Bushman, *et al.*, QIIME allows analysis of high-throughput community sequencing data, *Nat. Methods*, 2010, 7, 335–336.
- 43 Ohio Supercomputer Center, 1987.
- 44 T. Z. DeSantis, P. Hugenholtz, N. Larsen, M. Rojas, E. L. Brodie, K. Keller, T. Huber, D. Dalevi, P. Hu and G. L. Andersen, Greengenes, a chimera-checked 16S rRNA gene database and workbench compatible with ARB, *Appl. Environ. Microbiol.*, 2006, 72, 5069–5072.
- 45 S. F. Altschul, W. Gish, W. Miller, E. W. Myers and D. J. Lipman, Basic local alignment search tool, *J. Mol. Biol.*, 1990, 215, 403–410.
- 46 M. G. Langille, J. Zaneveld, J. G. Caporaso, D. McDonald, D. Knights, *et al.*, Predictive functional profiling of microbial communities using 16S rRNA marker gene sequences, *Nat. Biotechnol.*, 2013, 31, 814–821.
- 47 R. Caspi, R. Billington, L. Ferrer, H. Foerster, C. A. Fulcher, *et al.*, The MetaCyc database of metabolic pathways and enzymes and the BioCyc collection of pathway/genome databases, *Nucleic Acids Res.*, 2016, 44, D471–D480.
- 48 P. J. Mouser, A. L. N'Guessan, H. Elifantz, D. E. Holmes, K. H. Williams, M. J. Wilkins, P. E. Long and D. R. Lovley, Influence of heterogeneous ammonium availability on bacterial community structure and the expression of nitrogen fixation and ammonium transporter genes during

Paper

- in situ bioremediation of uranium-contaminated groundwater, *Environ. Sci. Technol.*, 2009, **43**, 4386–4392.
- 49 Groundwater Protection Council, Interstate Oil & Gas Conservation Commission, *FracFocus Chemical Disclosure Registry*, http://fracfocus.org, (accessed May 2017).
- 50 J. F. Gao, L. B. M. Ellis and L. P. Wackett, The University of Minnesota biocatalysis/biodegradation database: Improving public access, *Nucleic Acids Res.*, 2010, 38, D488–D491.
- 51 E. Otal and J. Lebrato, Anaerobic degradation of polyethylene glycol mixtures, *J. Chem. Technol. Biotechnol.*, 2003, **78**, 1075–1081.
- 52 Y. L. Huang, Q. B. Li, X. Deng, Y. H. Lu, X. K. Liao, M. Y. Hong and Y. Wang, Aerobic and anaerobic biodegradation of polyethylene glycols using sludge microbes, *Process Biochem.*, 2005, 40, 207–211.
- 53 F. Kawai, The biochemistry and molecular biology of xenobiotic polymer degradation by microorganisms, *Biosci., Biotechnol., Biochem.*, 2010, 74, 1743–1759.
- 54 M. Kanehisa, Y. Sato, M. Kawashima, M. Furumichi and M. Tanabe, KEGG as a reference resource for gene and protein annotation, *Nucleic Acids Res.*, 2016, 44, D457–D462.
- 55 R. A. Daly, M. A. Borton, M. J. Wilkins, D. W. Hoyt, D. J. Kountz, *et al.*, Microbial metabolisms in a 2.5-kmdeep ecosystem created by hydraulic fracturing in shales, *Nat. Microbiol.*, 2016, 1, 16146.
- 56 M. A. Cluff, A. Hartsock, J. D. MacRae, K. Carter and P. J. Mouser, Temporal changes in microbial ecology and

- geochemistry in produced water from hydraulically fractured Marcellus Shale gas wells, *Environ. Sci. Technol.*, 2014, **48**, 6508–6517.
- 57 J. Fichter, K. Wunch, R. Moore, E. Summer, S. Braman and P. Holmes, How Hot is Too Hot for Bacteria? A Technical Study Assessing Bacterial Establishment in Downhole Drilling, Fracturing and Stimulation Operations, in *NACE International Corrosion Conference*, National Association of Corrosion Engineers International, Salt Lake City, UT, March 11-15, 2012.
- 58 V. M. Pathak and Navneet, Review on the current status of polymer degradation: A microbial approach, *Bioresour. Bioprocess.*, 2017, 4(1), 15.
- 59 N. Obradors and J. Aguilar, Efficient biodegradation of high-molecular-weight polyethylene glycols by pure cultures of Pseudomonas stutzeri, *Appl. Environ. Microbiol.*, 1991, 57, 2383–2388.
- 60 M. Sugimoto, M. Tanabe, M. Hataya, S. Enokibara, J. A. Duine and F. Kawai, The first step in polyethylene glycol degradation by sphingomonads proceeds via a flavoprotein alcohol dehydrogenase containing flavin adenine dinucleotide, *J. Bacteriol.*, 2001, **183**, 6694–6698.
- 61 R. Marchal, E. Nicolau and J. P. Ballaguet, Biodegradability of polyethylene glycol 400 by complete microfloras, *Int. Biodeterior. Biodegrad.*, 2008, **62**, 384–390.
- 62 C. Han, R. Mwirichia, O. Chertkov, B. Held, A. Lapidus, *et al.*, Complete genome sequence of Syntrophobotulus glycolicus type strain (FlGlyR), *Stand. Genomic Sci.*, 2011, 4, 371–380.